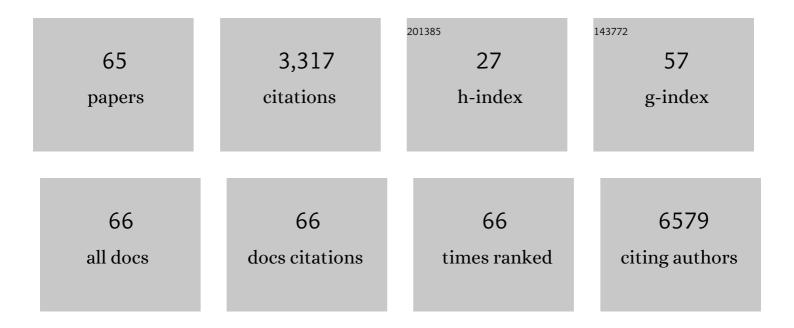
## Saikat Talapatra

List of Publications by Year in descending order

Source: https://exaly.com/author-pdf/1678804/publications.pdf Version: 2024-02-01



#	Article	IF	CITATIONS
1	Adsorption of Benzoic Acid: Structural Organization on the Surfaces of Pristine and Functionalized Single-Walled Carbon Nanotubes. ACS ES&T Water, 2021, 1, 251-258.	2.3	2
2	Photogating-driven enhanced responsivity in a few-layered ReSe <sub>2</sub> phototransistor. Journal of Materials Chemistry C, 2021, 9, 12168-12176.	2.7	7
3	In Vivo Partial Restoration of Neural Activity across Severed Mouse Spinal Cord Bridged with Ultralong Carbon Nanotubes. ACS Applied Bio Materials, 2021, 4, 4071-4078.	2.3	3
4	The influence of hydrostatic pressure and annealing conditions on the magnetostructural transitions in MnCoGe. Journal of Applied Physics, 2021, 129, .	1.1	9
5	Broadband photocurrent spectroscopy and temperature dependence of band gap of few-layer indium selenide (InSe). Emergent Materials, 2021, 4, 1029-1036.	3.2	7
6	Carbon Nanotube Based Robust and Flexible Solid-State Supercapacitor. ACS Applied Materials & Interfaces, 2021, 13, 56004-56013.	4.0	27
7	Electronic and optoelectronic properties of the heterostructure devices composed of two-dimensional layered materials. , 2020, , 151-193.		2
8	Label-free Electrochemical Detection of CGG Repeats on Inkjet Printable 2D Layers of MoS <sub>2</sub> . ACS Applied Materials & Interfaces, 2020, 12, 52156-52165.	4.0	15
9	2D Tungsten Chalcogenides: Synthesis, Properties and Applications. Advanced Materials Interfaces, 2020, 7, 2000002.	1.9	39
10	Magnetic field dependence of the martensitic transition and magnetocaloric effects in Ni49BiMn35In15. AIP Advances, 2020, 10, 015138.	0.6	1
11	Effects of magnetic and structural phase transitions on the normal and anomalous Hall effects in Ni-Mn-In-B Heusler alloys. Physical Review B, 2020, 101, .	1.1	24
12	High Adsorption of Benzoic Acid on Single Walled Carbon Nanotube Bundles. Scientific Reports, 2020, 10, 10013.	1.6	8
13	NMR studies of the ground states of Ni50-xCoxMn35In15 (x=1, 2.5) and Ni45Co5Mn37In13 Heusler alloys. AIP Advances, 2020, 10, 015328.	0.6	0
14	Influence of channel thickness on charge transport behavior of multi-layer indium selenide (InSe) field-effect transistors. 2D Materials, 2020, 7, 025030.	2.0	7
15	Role of layer thickness and field-effect mobility on photoresponsivity of indium selenide (InSe)-based phototransistors. Oxford Open Materials Science, 2020, 1, .	0.5	3
16	Gate-Induced Metal–Insulator Transition in 2D van der Waals Layers of Copper Indium Selenide Based Field-Effect Transistors. ACS Nano, 2019, 13, 13413-13420.	7.3	20
17	Electric Double Layer Field-Effect Transistors Using Two-Dimensional (2D) Layers of Copper Indium Selenide (CuIn7Se11). Electronics (Switzerland), 2019, 8, 645.	1.8	10
18	Adsorption of aromatic carboxylic acids on carbon nanotubes: impact of surface functionalization, molecular size and structure. Environmental Sciences: Processes and Impacts, 2019, 21, 2109-2117	1.7	6

SAIKAT TALAPATRA

#	Article	IF	CITATIONS
19	Fast photoresponse and high detectivity in copper indium selenide (Culn 7 Se 11 ) phototransistors. 2D Materials, 2018, 5, 015001.	2.0	24
20	High Performance Graphene-Based Electrochemical Double Layer Capacitors Using 1-Butyl-1-methylpyrrolidinium tris (pentafluoroethyl) trifluorophosphate Ionic Liquid as an Electrolyte. Electronics (Switzerland), 2018, 7, 229.	1.8	8
21	Low temperature photoconductivity of few layer <i>p</i> -type tungsten diselenide (WSe <sub>2</sub> ) field-effect transistors (FETs). Nanotechnology, 2018, 29, 484002.	1.3	11
22	High photoresponse of individual WS2 nanowire-nanoflake hybrid materials. Applied Physics Letters, 2018, 112, .	1.5	7
23	Viable route towards large-area 2D MoS <sub>2</sub> using magnetron sputtering. 2D Materials, 2017, 4, 021002.	2.0	40
24	Hydro-deoxygenation of CO on functionalized carbon nanotubes for liquid fuels production. Carbon, 2017, 121, 274-284.	5.4	14
25	Aligned carbon nanotube/zinc oxide nanowire hybrids as high performance electrodes for supercapacitor applications. Journal of Applied Physics, 2017, 121, .	1.1	35
26	Recent advances in investigations of the electronic and optoelectronic properties of group III, IV, and V selenide based binary layered compounds. Journal of Materials Chemistry C, 2017, 5, 11214-11225.	2.7	34
27	Adsorption energy of oxygen molecules on graphene and two-dimensional tungsten disulfide. Scientific Reports, 2017, 7, 1774.	1.6	62
28	Effect of underlying boron nitride thickness on photocurrent response in molybdenum disulfide - boron nitride heterostructures. Journal of Materials Research, 2016, 31, 893-899.	1.2	11
29	Laser THz Emission Spectroscopy of Gas Adsorption-Desorption Dynamics in Tungsten Disulfide Nanosheets. E-Journal of Surface Science and Nanotechnology, 2016, 14, 78-82.	0.1	2
30	Engineering Photophenomena in Large, 3D Structures Composed of Selfâ€Assembled van der Waals Heterostructure Flakes. Advanced Optical Materials, 2015, 3, 1551-1556.	3.6	17
31	Manganese oxide based Hybrid nanofibers for Supercapacitors. Materials Letters, 2015, 148, 142-146.	1.3	18
32	Chemical Vapor Deposition Synthesized Atomically Thin Molybdenum Disulfide with Optoelectronic-Grade Crystalline Quality. ACS Nano, 2015, 9, 8822-8832.	7.3	132
33	Ultrafast Intrinsic Photoresponse and Direct Evidence of Sub-gap States in Liquid Phase Exfoliated MoS2Thin Films. Scientific Reports, 2015, 5, 11272.	1.6	57
34	Fractional photo-current dependence of graphene quantum dots prepared from carbon nanotubes. Physical Chemistry Chemical Physics, 2015, 17, 24566-24569.	1.3	14
35	Phase diagram and magnetocaloric effects in Ni50Mn35(In1â^'xCrx)15 and (Mn1â^'xCrx)NiGe1.05 alloys. Journal of Applied Physics, 2014, 115, 17A922.	1.1	12
36	Electrochemical Characterization of Liquid Phase Exfoliated Two-Dimensional Layers of Molybdenum Disulfide. ACS Applied Materials & Interfaces, 2014, 6, 2125-2130.	4.0	121

SAIKAT TALAPATRA

#	Article	IF	CITATIONS
37	Temperature dependent electrical transport of disordered reduced graphene oxide. 2D Materials, 2014, 1, 011008.	2.0	86
38	Label-free as-grown double wall carbon nanotubes bundles for Salmonella typhimuriumimmunoassay. Chemistry Central Journal, 2013, 7, 102.	2.6	28
39	Tunable Electronics in Large-Area Atomic Layers of Boron–Nitrogen–Carbon. Nano Letters, 2013, 13, 3476-3481.	4.5	65
40	Magnetic properties and phase transitions of gadolinium-infused carbon nanotubes. Journal of Applied Physics, 2013, 113, .	1.1	5
41	Photosensor Device Based on Fewâ€Layered WS <sub>2</sub> Films. Advanced Functional Materials, 2013, 23, 5511-5517.	7.8	546
42	Conversion of Industrial Bio-Waste into Useful Nanomaterials. ACS Sustainable Chemistry and Engineering, 2013, 1, 619-626.	3.2	30
43	Sensors: Photosensor Device Based on Fewâ€Layered WS <sub>2</sub> Films (Adv. Funct. Mater. 44/2013). Advanced Functional Materials, 2013, 23, 5510-5510.	7.8	7
44	Carbon Nanotubes and Graphene Nanoribbons: Potentials for Nanoscale Electrical Interconnects. Electronics (Switzerland), 2013, 2, 280-314.	1.8	28
45	Effect of 1- Pyrene Carboxylic-Acid Functionalization of Graphene on Its Capacitive Energy Storage. Journal of Physical Chemistry C, 2012, 116, 20688-20693.	1.5	85
46	Transforming collagen wastes into doped nanocarbons for sustainable energy applications. Green Chemistry, 2012, 14, 1689.	4.6	65
47	Adsorption and Desorption of Chlorinated Compounds from Pristine and Thermally Treated Multiwalled Carbon Nanotubes. Journal of Physical Chemistry C, 2011, 115, 4552-4557.	1.5	35
48	Double resonance Raman study of disorder in CVD-grown single-walled carbon nanotubes. Carbon, 2011, 49, 1318-1325.	5.4	31
49	Application of Carbon Nanotubes for Removing Organic Contaminants from Water. Materials Express, 2011, 1, 183-200.	0.2	24
50	Understanding the Role of Sulfur in Tuning the Diameter and Morphology in the Chemical Vapor Deposition Growth of Carbon Nanotubes. Materials Express, 2011, 1, 160-166.	0.2	7
51	Stable Aqueous Dispersions of Noncovalently Functionalized Graphene from Graphite and their Multifunctional High-Performance Applications. Nano Letters, 2010, 10, 4295-4301.	4.5	449
52	Carbon nanotube-textured sand for controlling bioavailability of contaminated sediments. Nano Research, 2010, 3, 412-422.	5.8	11
53	Importance of Cr2O3 layer for growth of carbon nanotubes on superalloys. Carbon, 2010, 48, 844-853.	5.4	11
54	Investigating Photoinduced Charge Transfer in Carbon Nanotubeâ^'Peryleneâ^'Quantum Dot Hybrid Nanocomposites. ACS Nano, 2010, 4, 6883-6893.	7.3	55

SAIKAT TALAPATRA

#	Article	IF	CITATIONS
55	Electrochemical double layer capacitor electrodes using aligned carbon nanotubes grown directly on metals. Nanotechnology, 2009, 20, 395202.	1.3	80
56	Carbon Nanotubeâ^'MoS <sub>2</sub> Composites as Solid Lubricants. ACS Applied Materials & Interfaces, 2009, 1, 735-739.	4.0	128
57	Lüttinger Liquid to Al'tshulerâ~Aronov Transition in Disordered, Many-Channel Carbon Nanotubes. ACS Nano, 2009, 3, 207-212.	7.3	11
58	Air-assisted growth of ultra-long carbon nanotube bundles. Nanotechnology, 2008, 19, 455609.	1.3	66
59	Detection of Nanoscale Magnetic Activity Using a Single Carbon Nanotube. Nano Letters, 2008, 8, 4498-4505.	4.5	14
60	Ultralong Aligned Multi-Walled Carbon Nanotube for Electrochemical Sensing. Journal of Nanoscience and Nanotechnology, 2008, 8, 2085-2090.	0.9	9
61	First-Principles Study of Defect-Induced Magnetism in Carbon. Physical Review Letters, 2007, 99, 107201.	2.9	170
62	Aligned Carbon Nanotubeâ^'Polymer Hybrid Architectures for Diverse Flexible Electronic Applications. Nano Letters, 2006, 6, 413-418.	4.5	306
63	Charge-injection-induced dynamic screening and origin of hysteresis in field-modulated transport in single-wall carbon nanotubes. Applied Physics Letters, 2006, 89, 162108.	1.5	65
64	Quantitative analysis of hysteresis in carbon nanotube field-effect devices. Applied Physics Letters, 2006, 89, 132118.	1.5	53
65	Gas Adsorption on HiPco Nanotubes:Â Surface Area Determinations, and Neon Second Layer Data. Nano Letters, 2004, 4, 1133-1137.	4.5	38